

Field-induced orbital order-disorder transition in an *A*-type antiferromagnetic manganite: High-field study of $\text{Nd}_{0.45}\text{Sr}_{0.55}\text{MnO}_3$

T. Hayashi and N. Miura

Institute for Solid State Physics, University of Tokyo, Kashiwa 277-8581, Japan

K. Noda

The Department of Physics, Sophia University, Tokyo 102-8554, Japan

H. Kuwahara

*The Department of Physics, Sophia University, Tokyo 102-8554, Japan
and PRESTO, JST, Japan*

S. Okamoto,* S. Ishihara,† and S. Maekawa

Institute for Materials Research, Tohoku University, Sendai 980-8577, Japan

(Received 23 May 2001; published 12 December 2001)

Magnetization and magnetoresistance were measured in *A*-type antiferromagnet $\text{Nd}_{0.45}\text{Sr}_{0.55}\text{MnO}_3$ utilizing pulsed magnetic fields up to 45 T. We have observed a ferromagnetic transition accompanied by a discontinuous decrease of resistivity. The temperature dependence of the resistivity in the ferromagnetic state showed characteristics of a three-dimensional metal. The observed phenomena are explained in terms of simultaneous destruction of the $d_{x^2-y^2}$ orbital ordering and the *A*-type antiferromagnetic spin ordering by magnetic field.

DOI: 10.1103/PhysRevB.65.024408

PACS number(s): 75.30.Kz, 72.15.Gd, 75.30.Vn

I. INTRODUCTION

Recent studies for perovskite manganites $R_{1-x}A_x\text{MnO}_3$ have revealed the importance of interplay among the spin, charge, lattice, and orbital degree of freedom. The colossal magnetoresistance effect in the vicinity of ferromagnetic transition of ferromagnetic metallic manganites is generally explained by the double-exchange model which has been developed by several researchers since it was first proposed in the 1950's (Refs. 1–3). However, the recent findings of various phenomena in the transport, magnetic, and structural properties have revealed many more competing effects such as orbital degree of freedom, Coulomb repulsive interaction, Jahn-Teller effect, or the superexchange interaction.^{4,5} A rich variety of magnetic structures have been found in many manganites^{6,7} and correspondingly many theoretical models have been proposed to explain the phase diagram.^{8–10} An exciting physics is underlying not only in the ground state, but also in some of the excited states under different external parameters such as temperature, magnetic field, and pressure. One of the most remarkable phenomena under magnetic fields is a field-induced metal-insulator transition observed in slightly doped manganite $\text{La}_{1-x}\text{Sr}_x\text{MnO}_3$ ($x \sim 1/8$) (Refs. 11,12). This transition is ascribed to the orbital antiferromagnetic ordering transition.^{10,12} For the ferromagnetic metallic state in a moderately doped region, neither anisotropic conductivity nor anisotropic spin excitation have been observed. In order to explain these phenomena, a possibility of orbital liquid has been proposed.¹³ With increasing doping of divalent ions, the magnetic structure of the ground state becomes an *A*-type antiferromagnet while the transport properties remain metallic.¹⁴ It is theoretically predicted that this spin ordering is accompanied by the $d_{x^2-y^2}$ -type ferromagnetic orbital ordering (OO).^{8,10}

$\text{Nd}_{0.45}\text{Sr}_{0.55}\text{Mn}_3$ is a typical *A*-type antiferromagnetic metallic manganite whose Néel temperature is around 220 K (Ref. 7). Corresponding to the antiferromagnetic transition, a structural transition takes place and the two-dimensional transport properties are enhanced.¹⁵ From such behavior it is thought that the antiferromagnetic transition is accompanied by the $d_{x^2-y^2}$ -type OO, that is ascribed to the orbital disorder-order transition. The appearance of the *A*-type antiferromagnetism has been predicted by different models taking account of orbital degeneracy. To clarify the mechanism of the *A*-type AF (antiferromagnetic) ordering, it is important to study the effect of external magnetic fields.

In this paper, we report the magnetic and transport properties of $\text{Nd}_{0.45}\text{Sr}_{0.55}\text{MnO}_3$ in high magnetic fields. Measurements of magnetization and magnetoresistance have been carried out over a wide temperature range. We have observed a new type of metamagnetic transition that is accompanied by a dimensional transition of the transport properties. The observed phenomena indicate that a destruction of the orbital-ordered phase is caused by external magnetic fields, accompanying a simultaneous diminishing of the *A*-type spin ordering.

II. EXPERIMENT

Single crystals of $\text{Nd}_{0.45}\text{Sr}_{0.55}\text{MnO}_3$ were grown by the floating-zone method, details of which were almost the same as described in Ref. 16. In order to check the quality of the grown crystals, Rietveld refinement of powder x-ray-diffraction patterns for the pulverized crystal indicated that no impurity phase was contained. (The crystallographic axis was not specified.) Pulsed magnetic fields up to 45 T were generated in a duration time of about 40 ms using a nondestructive long-pulse magnet energized by a capacitor bank

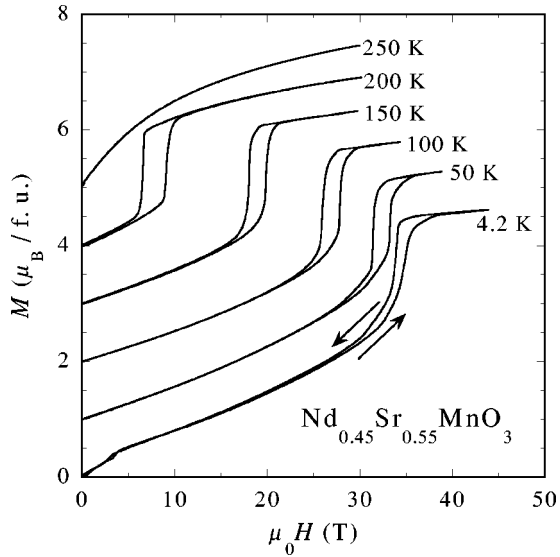


FIG. 1. M - H curves of $\text{Nd}_{0.45}\text{Sr}_{0.55}\text{MnO}_3$ at various temperatures. For each curve the origin is shifted by $1 \mu_B/\text{f.u.}$ for clarity.

with the maximum stored energy of 900 kJ. For magnetization measurements, we applied the induction method using a pair of coaxial pickup coils. To obtain magnetization, the voltage induced in the pickup coils was recorded by a 14-bit transient recorder with a sampling time of $5 \mu\text{s}$ and integrated numerically. Transport measurements were carried out by using the standard four-probe method with a dc current of about $100 \mu\text{A}$.

III. RESULTS AND DISCUSSION

The M - H curves of $\text{Nd}_{0.45}\text{Sr}_{0.55}\text{MnO}_3$ measured between 4.2 K and 250 K are shown in Fig. 1. For each curve in this figure, the origin is shifted by $1 \mu_B/\text{f.u.}$ for clarity. At a temperature above $T_N \sim 220$ K, the M - H curve shows a paramagnetic behavior with a rapid increase of M in the low-field region due to the ferromagnetic fluctuation. Below T_N down to the lowest temperature it shows a metamagnetic transition at some critical fields. As the M - H curve after the metamagnetic transition is very linear between 36–45 T at 4.2 K, we can obtain the fictitious spontaneous magnetization of the forced ferromagnetic phase M_0 by linearly extrapolating to the zero field. It should be noted that M_0 at 4.2 K is about $4.2 \mu_B$, which is much larger than the saturation moment of an average Mn ion moment ($3.45 \mu_B$). Assuming that the spin of Mn ions is fully polarized in the ferromagnetic state, the moment of a Nd ion at the ground state is estimated to be $1.7 \mu_B$. We can thus envisage that the paramagnetic behavior at 4.2 K in the low-field region is caused by the Nd moment. Except for this paramagnetic behavior, all M - H curves below T_N show ferromagnetic transition and the nearly linear field dependence with an almost temperature-independent susceptibility below the transition fields.

Figure 2(a) shows the magnetoresistance of $\text{Nd}_{0.45}\text{Sr}_{0.55}\text{MnO}_3$ taken at various temperatures. Below the ferromagnetic transition field, the resistivity ρ decreases

monotonically with increasing the field. At the ferromagnetic transition, ρ suddenly drops and becomes nearly field independent above the transition field. Figure 2(b) shows the temperature dependence of ρ at constant magnetic fields. All the points shown in this figure were taken from field-increasing process. The kink on the ρ - T curve corresponds to T_N for each magnetic field. It is clearly seen that T_N gradually decreases with increasing the fields. At each field, the temperature dependence below T_N is qualitatively the same as that of zero field, where two-dimensional transport phenomena have been observed.¹⁵ Above T_N , however, the resistivity shows normal metallike temperature dependence. A striking feature of the transport properties is seen in Fig. 2(c), where the resistivity is plotted as a function of the square of temperature at each field in the ferromagnetic state. It is seen that the resistivity in the ferromagnetic state is almost proportional to T^2 at each field, as in usual three-dimensional itinerant ferromagnets. The T^2 dependence in the ferromagnetic phase is in sharp contrast to the peculiar temperature dependence in the AF phase, which is considered to be a two-dimensional metal.¹⁵ From the observed phenomena, we can deduce that the ferromagnetic transition is accompanied by the dimensional crossover of the transport properties.

From the observed transition points the magnetic phase diagram is determined as shown in Fig. 3. Circles and squares stand for the transition fields in the field-increasing and field-decreasing processes, respectively. Because the phase above T_N is paramagnetic at zero field, there should be the phase boundary between the paramagnetic state and the ferromagnetic state at high temperatures, although it could not be identified in the present study. The ferromagnetic transition field linearly increases with decreasing temperature, and approaches to a constant value in the low-temperature region. This tendency is qualitatively similar to that of the transition from the charge- and orbital-ordered phase to the ferromagnetic metallic phase observed in many different kinds of manganites with $x \sim 0.5$ (Refs. 17,18). As for the hysteretic behavior, however, there are considerable differences from the case of charge-ordered manganites. For the transition in $\text{Nd}_{0.45}\text{Sr}_{0.55}\text{MnO}_3$, the hysteretic region is very small compared with that of the crystalline orbital ferromagnetic (CO-FM) transition. Moreover, the magnitude of the hysteresis loop at the transition in $\text{Nd}_{0.45}\text{Sr}_{0.55}\text{MnO}_3$ is almost temperature independent, in contrast to the latter transition.

Ferromagnetic transitions have been observed in many other manganites with $x \sim 0.5$, that are phenomenologically understood as a result of a competition between the charge ordering instability and the double-exchange interaction. For samples in the present work, however, no charge ordering has been observed. Since the magnetic anisotropy energy K in $\text{Nd}_{0.45}\text{Sr}_{0.55}\text{MnO}_3$ is very small (less than 0.3 meV) compared with the exchange $J_{12g} \sim 1.5$ meV,²² it is unlikely for the system to undergo a metamagnetic transition as in a usual antiferromagnetic substance. Therefore, the observed metamagnetic transition suggests that the remaining degree of freedom, the orbital must play a critical role.

Let us focus on the orbital degree of freedom in a Mn ion

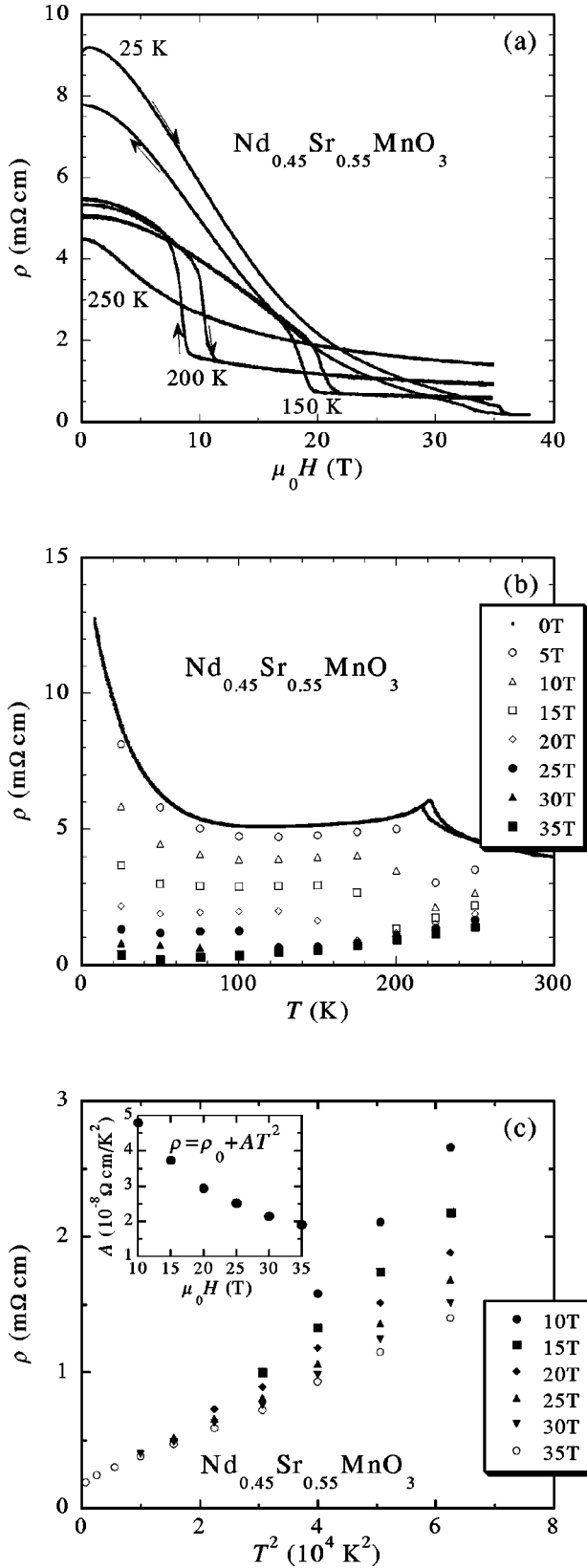


FIG. 2. (a) Magnetoresistance of $\text{Nd}_{0.45}\text{Sr}_{0.55}\text{MnO}_3$. (b) Temperature dependence in $\text{Nd}_{0.45}\text{Sr}_{0.55}\text{MnO}_3$ at various fields. The data are taken from field-increasing process. (c) Resistivity in the ferromagnetic state as a function of T^2 . The inset shows field dependence of the coefficient A defined as $\rho = \rho_0 + AT^2$.

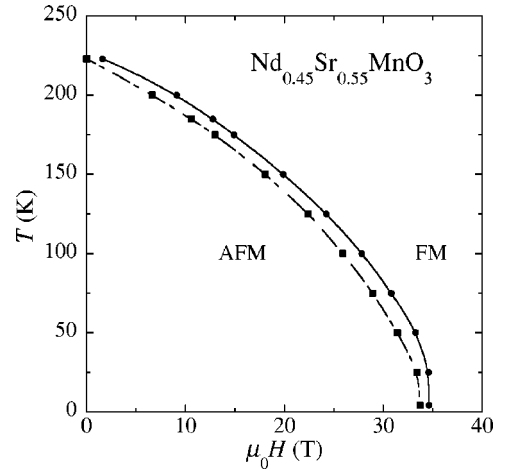


FIG. 3. Phase diagram of $\text{Nd}_{0.45}\text{Sr}_{0.55}\text{MnO}_3$. Circles and squares stand for transition fields of field-increasing and field-decreasing process, respectively.

and explain theoretically the observed metamagnetic transition. We consider the following model, where the doubly degenerate e_g orbitals and a localized spin for the t_{2g} electrons are introduced at each Mn site in a simple cubic lattice:⁵

$$\mathcal{H} = \sum_{\langle ij \rangle \gamma \gamma' \sigma} (t_{ij}^{\gamma \gamma'} \tilde{d}_{i\gamma\sigma}^\dagger \tilde{d}_{j\gamma'\sigma} + \text{H. c.}) - J_H \sum_i \vec{S}_i \cdot \vec{S}_{ii} + J_t \sum_{\langle ij \rangle} \vec{S}_{ii} \cdot \vec{S}_{ij} + \mathcal{H}_J. \quad (1)$$

The first term describes the hopping of the e_g electron between the nearest-neighboring (NN) sites. Here, $\tilde{d}_{i\gamma\sigma}$ is the annihilation operator of the e_g electron at site i with spin σ and orbital γ , and excludes a doubly occupied state of electron due to the strong Coulomb interaction.¹⁹ The transfer integral $t_{ij}^{\gamma \gamma'}$ is determined by the Slater-Koster formula.²⁰ The second and third terms describe the Hund coupling (J_H) between the e_g spin \vec{S}_i ($S=1/2$) and the t_{2g} spin \vec{S}_{ii} ($S=3/2$), and the AF interaction (J_t) between the NN t_{2g} spins, respectively. The last term is derived by the second-order processes of the electron hopping under the strong Coulomb interactions

$$\mathcal{H}_J = -2J_1 \sum_{\langle ij \rangle} \left(\frac{3}{4} n_i n_j + \vec{S}_i \cdot \vec{S}_j \right) \left(\frac{1}{4} - \tau_i^l \tau_j^l \right) - 2J_2 \sum_{\langle ij \rangle} \left(\frac{1}{4} n_i n_j - \vec{S}_i \cdot \vec{S}_j \right) \left(\frac{3}{4} + \tau_i^l \tau_j^l + \tau_i^l + \tau_j^l \right), \quad (2)$$

where $\tau_i^l = \cos(2\pi m_l/3)T_{iz} - \sin(2\pi m_l/3)T_{ix}$ with $(m_x, m_y, m_z) = (1, 2, 3)$. l denotes the direction of the bond connecting site i with site j . Here, \vec{T}_i is the pseudospin operator for the orbital degree of freedom given by $\vec{T}_i = \frac{1}{2} \sum_{\gamma \gamma' \sigma} \tilde{d}_{i\gamma\sigma}^\dagger \vec{\sigma}_{\gamma \gamma'} \tilde{d}_{i\gamma'\sigma}$ with the Pauli matrices $\vec{\sigma}$, and n_i is the number operator of the e_g electron. This term describes the interactions between NN spins and orbitals and their

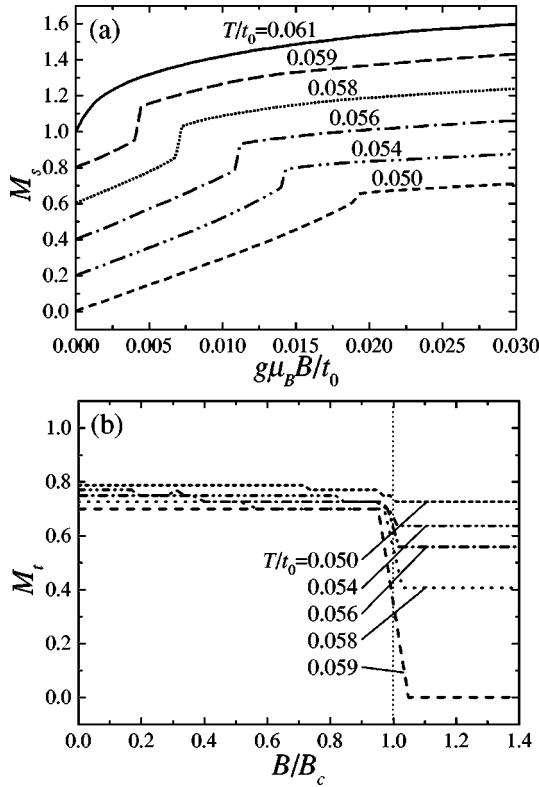


FIG. 4. Theoretical results of the magnetic-field dependence of (a) the ferromagnetic-order parameter M_s and (b) the orbital-order parameter M_t for the uniform $d_{x^2-y^2}$ -type OO state. g and μ_B indicate the g factor and the Bohr magneton, respectively. A magnitude of the applied magnetic field $g\mu_B B/t_0=0.01$ corresponds to about 20 T for $t_0=0.5$ eV and $g=2$. The parameter values are chosen to be $J_1/t_0=0.25$, $J_2/t_0=0.075$, $J_t/t_0=0.007$, and $x=0.8$. In (a), the vertical scales are shifted by 0.2 for clarity.

magnitudes are denoted by J_1 and J_2 . The spin- and orbital-order parameters are calculated by the mean-field approximation at finite hole concentration (x) and temperature (T). A detailed derivation of the Hamiltonian and the formulation is presented in Refs. 5 and 10. It has been shown that the model and the mean-field approximation well describe the magnetic and orbital states in the actual compounds.

The magnetic-field dependence of the (ferromagnetic) FM-order parameter M_s and the order parameter for the uniform $d_{x^2-y^2}$ -type OO state M_t are presented in Fig. 4. We define $M_s = \langle \vec{S}_i \cdot \vec{B} \rangle / (|\vec{S}_i| |\vec{B}|)$, where \vec{B} is a magnetic field and $\langle \cdots \rangle$ implies the thermal average, and $M_t = -\langle T_{iz} \rangle / |\vec{T}_i|$. The energy parameters are chosen to be $J_1 = 0.25$, $J_2 = 0.075$, and $J_t = 0.007$ in units of t_0 , which is the transfer integral between the $d_{3z^2-r^2}$ orbitals in the z direction and is estimated to be about 0.5 eV. In order to reproduce the A-type AF order at $T=0$, x is chosen to be 0.8 that is somewhat larger than that in the actual compounds. This point may be improved by taking into account the orbital fluctuation,¹³ which shifts the phase boundary between the FM and A-type AF phases to the lower x region.²¹ However, the qualitative behavior for the calculated results is robust. Above the Néel temperature ($T_N=0.06t_0$), M_s monotonically increases with increasing B . Below T_N , there exists a

discontinuous jump in the magnetization curve at a critical magnetic field B_c . As shown in Fig. 4(b), this is accompanied with a sudden change of the orbital state; a magnitude of the $d_{x^2-y^2}$ -type OO is reduced discontinuously at B_c . It is shown in Fig. 4(a) that B_c gradually increases with decreasing T . We suppose that the obtained discontinuous jump in the magnetization curve corresponds to the metamagnetic transition observed in $\text{Nd}_{0.45}\text{Sr}_{0.55}\text{MnO}_3$ (Fig. 1). A mechanism of this transition is the following; as is well known, the A-type AF order and the $d_{x^2-y^2}$ -type OO are stabilized cooperatively. This is because both the two favor the electron hopping in the x - y plane and prohibit the hopping in the z direction. By applying the magnetic field, a spin canting is raised. Then, the obstruction of the electron hopping due to the AF spin alignment is relaxed and the $d_{x^2-y^2}$ -type OO becomes weaker simultaneously. With increasing the magnetic field, a transition from the orbital-ordered A-type AF phase to the FM phase, where the orbital is weakly ordered occurs at B_c . When the orbital fluctuation discussed above is taken into account in the calculation, it is expected that the OO in the FM phase is inconspicuous and the discontinuous changes of the magnetic and orbital states at B_c become more remarkable. At low temperatures, since the spin- and orbital-order parameters are almost saturated, a high magnetic field is required to collapse this ordered phase. The M - H curve (Fig. 1) suggests that the transition is of first order. Although the hysteresis is not reproduced in Fig. 4(a), the theoretical model predicts the first-order transition.¹⁰ We note that the magnetic-field-dependent OO state is also observed in $\text{La}_{1-x}\text{Sr}_x\text{MnO}_3$ with $x \sim 1/8$. However, unlike the present case, the magnetic field stabilizes the OO phase, since the OO and FM phases are cooperatively realized in $\text{La}_{7/8}\text{Sr}_{1/8}\text{MnO}_3$.^{12,10}

Finally, we discuss the transport properties in the ferromagnetic state. As shown in Fig. 2(c), the resistivity (ρ) in the ferromagnetic state is almost proportional to T^2 at each field, i.e., $\rho = AT^2$ with A being a constant. Such a temperature dependence of the resistivity has been observed in many kinds of ferromagnetic metallic manganites at zero field.^{6,23} These phenomena are usually interpreted as an electron-electron scattering. However, if the Fermi liquid picture is applied to the system, the coefficient A is too large compared with the value expected from the coefficient of the specific heat γ (Ref. 24). As regards the T^2 dependence, there has been a considerable controversy. Jaime *et al.* attribute it to single magnon scattering due to the thermally destroyed half-metallic state.²⁵ Zhao *et al.* propose a small-polaron metallic conduction mechanism.²⁶ It should be noted that in the experimental results observed in this work, the coefficient A has a negative-field dependence as illustrated in the inset of Fig. 2(c). A similar behavior has been reported by Mandal *et al.*²⁷ This negative-field dependence of A implies that the dominant carrier scattering mechanism in the ferromagnetic state is electron-magnon scattering caused by thermally excited minority-spin states. It should be emphasized that the ferromagnetic phase is considered as an orbital liquid state. The detailed temperature and field dependence of the resistivity will be discussed elsewhere.

IV. SUMMARY

We have performed measurements of magnetization and magnetoresistance for the layered antiferromagnet $\text{Nd}_{0.45}\text{Sr}_{0.55}\text{MnO}_3$ by means of pulsed magnetic fields up to 45 T. It was found that the first-order ferromagnetic transition occurs with a small hysteresis below T_N . These phenomena indicate that the transition is ascribed to the collapse of the $d_{x^2-y^2}$ OO as well as the collapse of the A-type AF spin ordering.

ACKNOWLEDGMENTS

The authors would like to thank R. Maezono and M. Tokunaga for helpful discussions. They also thank K. Uchida and Y. H. Matsuda for experimental supports. This work was partly performed using a nondestructive magnet developed by K. Kindo. The part of the work was supported by Priority-Areas Grants from the Ministry of Education, Science and Culture, and Sports of Japan.

*Present address: The Institute of Physical and Chemical Research (RIKEN), Saitama, 351-0198, Japan.

†Present address: Department of Applied Physics, University of Tokyo, Tokyo, 113-8656, Japan.

¹C. Zener, *Phys. Rev.* **82**, 403 (1951).

²P. W. Anderson and H. Hasegawa, *Phys. Rev.* **100**, 675 (1955).

³N. Furukawa, *J. Phys. Soc. Jpn.* **64**, 2734 (1995).

⁴A. J. Millis, P. B. Littlewood, and B. J. Shraiman, *Phys. Rev. Lett.* **74**, 5144 (1995).

⁵S. Ishihara, J. Inoue, and S. Maekawa, *Phys. Rev. B* **55**, 8280 (1997).

⁶A. Urushibara, Y. Moritomo, T. Arima, A. Asamitsu, G. Kido, and Y. Tokura, *Phys. Rev. B* **51**, 14 103 (1995).

⁷H. Kawano, R. Kajimoto, H. Yoshizawa, Y. Tomioka, H. Kuwahara, and Y. Tokura, *Phys. Rev. Lett.* **78**, 4253 (1997).

⁸R. Maezono, S. Ishihara, and N. Nagaosa, *Phys. Rev. B* **58**, 11 583 (1998).

⁹J. van den Brink and D. Khomskii, *Phys. Rev. Lett.* **82**, 1016 (1999).

¹⁰S. Okamoto, S. Ishihara, and S. Maekawa, *Phys. Rev. B* **61**, 14 647 (2000).

¹¹H. Nojiri, K. Kaneko, M. Motokawa, K. Hirota, Y. Endoh, and K. Takahashi, *Phys. Rev. B* **60**, 4142 (1999).

¹²Y. Endoh, K. Hirota, S. Ishikawa, S. Okamoto, Y. Murakami, S. Nishizawa, T. Fukuda, H. Kimura, H. Nojiri, K. Kaneko, and S. Maekawa, *Phys. Rev. Lett.* **82**, 4328 (1999).

¹³S. Ishihara, M. Yamanaka, and N. Nagaosa, *Phys. Rev. B* **56**, 686 (1997).

¹⁴T. Akimoto, Y. Maruyama, Y. Moritomo, A. Nakamura, K. Hirota, K. Ohoyama, and M. Ohashi, *Phys. Rev. B* **57**, R5594 (1998).

¹⁵H. Kuwahara, T. Okuda, Y. Tomioka, A. Asamitsu, and Y. Tokura, *Phys. Rev. Lett.* **82**, 4316 (1999).

¹⁶H. Kuwahara, Y. Moritomo, Y. Tomioka, A. Asamitsu, M. Kasai, R. Kumai, and Y. Tokura, *Phys. Rev. B* **56**, 9386 (1997).

¹⁷H. Kuwahara, Y. Tomioka, A. Asamitsu, Y. Moritomo, and Y. Tokura, *Science* **270**, 961 (1995).

¹⁸M. Tokunaga, N. Miura, Y. Tomioka, and Y. Tokura, *Phys. Rev. B* **57**, 5259 (1998).

¹⁹T. Saitoh, A. E. Bocquet, T. Mizokawa, H. Namatame, A. Fujimori, M. Abbate, Y. Takeda, and M. Takano, *Phys. Rev. B* **51**, 13 942 (1995).

²⁰J. C. Slater and G. F. Koster, *Phys. Rev.* **94**, 1498 (1954).

²¹M. van Veenendaal and A. J. Fedro, *Phys. Rev. B* **59**, 1285 (1999).

²²H. Yoshizawa, H. Kawano, J. A. Fernandez-Baca, H. Kuwahara, and Y. Tokura, *Phys. Rev. B* **58**, R571 (1998).

²³G. J. Snyder, R. Heikes, S. DiCarolis, M. R. Beasley, and T. H. Geballe, *Phys. Rev. B* **53**, 14 434 (1996).

²⁴T. Okuda, A. Asamitsu, Y. Tomioka, T. Kimura, and Y. Tokura, *Phys. Rev. Lett.* **81**, 3203 (1998).

²⁵M. Jaime, P. Lin, M. B. Salamon, and P. D. Han, *Phys. Rev. B* **58**, R5901 (1998).

²⁶Guo-meng Zhao, V. Smolyaninova, W. Prellier, and H. Keller, *Phys. Rev. Lett.* **84**, 6086 (2000).

²⁷P. Mandal, K. Bärner, L. Haupt, A. Poddar, R. von Helmolt, A. G. M. Jansen, and P. Wyder, *Phys. Rev. B* **57**, 10 256 (1998).